807. Wavelet transform and current signature analysis for welding machine measurement

Ramazan Caglar
Department of Electrical Engineering, Istanbul Technical University Sariyer, Istanbul, Turkey
E-mail: *caglarr@itu.edu.tr*

(Received 3 May 2012; accepted 14 May 2012)

Abstract. This study aims to extract the stationary features from a non-stationary data using continuous wavelet transform. For this purpose a Hall effect sensor is used to obtain current measurements during the welding operation. A welding process includes several stages referred to as the initial case, transient case and operation case. In this manner, some frequency components can be determined for these cases thereby defining behavior of a particular welding machine. Regarding to the wavelet analysis results, fundamental frequency at 50 Hz is determined to be a dominant characteristic for the considered application. Moreover, side band effects are observed around the fundamental frequency. A sinusoidal waveform of 50 Hz is localized with huge amplitude values in very short time of the time-scale plane and this duration is required during the welding operation in terms of contact between the electrode and material surface.

Keywords: wavelet analysis, feature extraction, electric arc welding machine, Hall effect sensors, vibration.

1. Introduction

An electric arc formed by a welding power source can be considered as a transformation of electrical energy to heat energy, which is required during the arc welding. The arc welding involves low-voltage, high-current arcs between the electrode and material as a work-piece [1]. Some important applications of the electric arcs in which it is desirable to know the arc parameters accurately are in arc welding, plasma torches, switchgear, and arc furnaces [2, 3].

All electric welding machines perform the same function regardless of their size: they melt pieces of metal in order to mechanically bond them together [4-7]. They generate a low voltage AC at high amperage. The voltage range is between 24 and 50 volts AC while the current value changes from 20 amperes to as high as 500 amperes. Effect of the high current appears by blue arc in welding. This arc at high temperature heats up the metal and then it melts a puddle of molten metal.

The most common welder used in industrial is the arc welder. This type of electric machine uses a stick electrode to conduct the electricity to sample material and hence it melts at the same time to fill in the gaps. A wire feed machine uses a roll of wire and the wire feeds into the blue arc and fills in the gap between the two pieces of metal. A Tungsten Inert Gas (TIG) machine or welder uses a tungsten tip which creates the high temperature needed in the welding process. Along with the arc, an inert gas such as argon is fed into the TIG welding puddle of metal to remove any impurities that come from the surrounding environment [6, 8].

In recent years, a great deal of the research on spectra of welding plasma has been undertaken considering the acquisition of spectrum signal and practical applications in monitoring the welding quality [8-10]. Also, signal properties of the laser-based welding system have been studied in the spectral domain [8, 11] as well as neural network application [11]. Other applications of the spectral analysis for the welding processes have been focused on detection and feature extraction techniques as indicated in the references [8, 13-17]. Whereas, one of the most powerful data analyzing techniques is wavelet transform and its applications to welding processes can be interpreted as an open problem in terms of the related literature.

Hence, as an alternative approach presented in this study, time-scale properties of the current signal of an electric arc welding machine are examined under the continuous wavelet transform and a stationary signal part at 50 Hz is extracted from the non-stationary welding current to determine the welding duration.

2. Mathematical methods

In terms of the mathematical tools, two different approaches are considered under this title. The first one is wavelet transform, which is suitable for the non-stationary signals and the second one is also power spectrum approach that can be used for stationary signals.

2. 1. Wavelet transform

The use of wavelet transform is particularly appropriate since it gives information about the signal both in frequency and time domains. Let $f(x)$ be the signal, the continuous wavelet transform of $f(x)$ is then defined as:

$$W_f(a,b) = \int_{-\infty}^{+\infty} f(x) \cdot \psi_{a,b}(x) \cdot dx \tag{1}$$

where:

$$\psi_{a,b}(x) = \frac{1}{\sqrt{|a|}} \psi\left(\frac{x-a}{a}\right) \qquad a, b \in \Re,\ a \neq 0 \tag{2}$$

and it provides the admissibility condition as below:

$$C_\psi = \int_0^{+\infty} \frac{|\psi(\omega)|^2}{\omega} d\omega < \infty \tag{3}$$

and for this reason, it is:

$$\int_{-\infty}^{+\infty} \psi(x) \cdot dx = 0 \tag{4}$$

Here $\psi(\omega)$ stands for the Fourier transform of $\psi(x)$. The admissibility condition implies that the Fourier transform of $\psi(x)$ vanishes at the zero frequency. Therefore ψ is called as a wave or the mother wavelet and it have two characteristic parameters, namely, dilation (a) and translation (b), which vary continuously. The translation parameter, "b", controls the position of the wavelet in time. A "narrow" wavelet can access high-frequency information, while a more dilated wavelet can access low-frequency information. This means that the parameter "a" varies with different frequency. The parameters "a" and "b" take discrete values, $a = a_0^j$, $b = nb_0a_0^j$, where $n, j \in Z$, $a_0 > 1$, and $b_0 > 0$. The discrete wavelet transformation (DWT) is defined as [18-20]:

$$DWT[j,k]=\frac{1}{\sqrt{a_0^j}}\sum_n f[n]\psi\left[\frac{k-na_0^j}{a_0^j}\right] \tag{5}$$

2. 2. Auto-power spectral density

A common approach for extracting the information about the frequency features of a random signal is to transform the signal to the frequency domain by computing the Discrete Fourier Transform (DFT). For a block of data of length N samples, the transform at frequency $m\Delta f$ is given by:

$$X(m\Delta f)=\sum_{k=0}^{N-1} x(k\Delta t)\cdot e^{-j2k\pi m/N} \tag{6}$$

where Δf is the frequency resolution and Δt is the data-sampling interval. The auto-power spectral density (APSD) or Power Spectral Density (PSD) of $x(t)$ is estimated as:

$$S_{xx}(f)=\frac{1}{N}\left|X(m\Delta f)\right|^2,\ f=m\Delta f \tag{7}$$

The cross-power spectral density (CPSD) between $x(t)$ and $y(t)$ is similarly estimated. The statistical accuracy of the estimate in Equation (3) increases as the number of data points or the number of blocks of data increases.

3. Measurement system and data acquisition

In this study, the measurement of the primer current drawn by the welder is realized by the help of a linear Hall effect sensor. Sensor should be placed at an air gap which is formed over the coil in order to detect the current. Primer coil may be composed of multiple turns as well as it can be used as only one winding (conductive element carrying the current directly passes through coil) as presented in Fig. 1. Due to Hall effect the magnetic flux generated by primer current in toroid produces voltage proportional to the flux density at the ends of the sensor [8, 22-24].

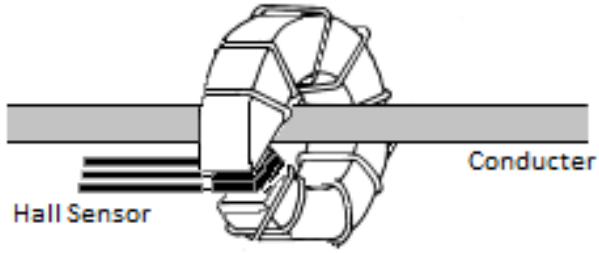

Fig. 1. Current measurement with Hall effect sensor [12]

For this application, the linear Hall effect sensor of A3516 Allegro Company is used. A3516 has a sensitivity of 2.5×10^4 mV/T (2.5 mV/G). Operational voltage interval of the sensor is between 4.5 V and 5.5 V while its nominal operational voltage is 5 V. Operational magnetic flux density interval of the sensor is ± 80 mT (± 800 G) and it can operate at temperatures between -40 ^{0}C and +150 ^{0}C [8, 24, 27].

In order to get the data acquisition, Hall effect sensor type current transformer is connected to the primary side of the welding machine. This sensor output is directed to the computer system through the PCI hardware, which is multifunction type of Advantech 1716L, with sampling rate of 0.005 sec., and then the collected data is analyzed by MATLAB program. For this purpose, considered measurement and data collection system is shown in Fig. 2.

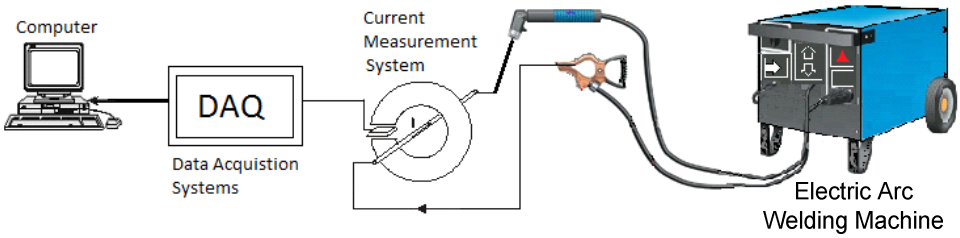

Fig. 2. Measurement system for welding

Hence, the data to be used in this study is collected during the welding process of two steel work-pieces by an electrical arc welding machine (model ESAB-LHE 260). In this study, the welding process is applied to ST37 steel by "rutile" basis electrode using Metal Active Gas (MAG) method. Some specific properties of this welder are listed as below:

- Frequency: 50/60 Hz.
- Number of phases: 3~ AC.
- Primer: 100 VA, Voltage: 440 V-220 V-240 V.
- Primer current: 17/29 A.
- Secondary: 55 V (DC), 100 %: 200 A – 35 %: 315 A.

4. Feature extraction and current signature analysis based on wavelet transform

Current variation, which is provided from the measurement system, is shown in Fig. 3. There are three regions of the current variation. The first part is related to the initial case, before the operation. The second one is the transient case and the third one is due to the operation case of the welding. In this manner the following figure shows the overall current variation in time domain.

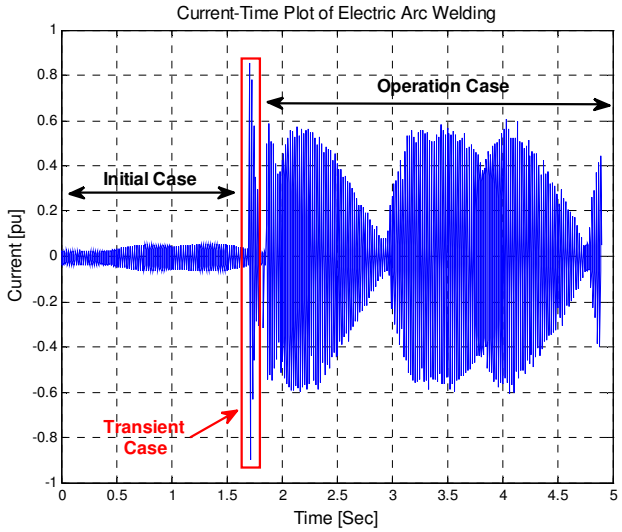

Fig. 3. Overall current variation of the welder (1 pu = 144.75 A)

The overall current variation of the welder in Fig. 3 represents a non-stationary signal. Therefore, one of the suitable mathematical tools to analyze this signal is the wavelet transform as well as short-time Fourier transform. For this reason, if the Continuous Wavelet Transform (CWT), which is defined as given in Equation 1, is applied to this measurement, its time-scale-amplitude variation can be presented by Fig. 4.

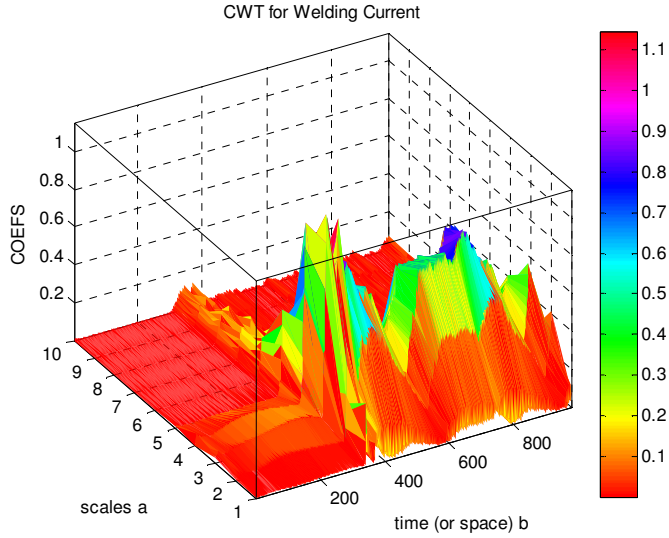

Fig. 4. CWT welding current (time = b × 0.005 s)

As seen in Fig. 4 the computation of the CWT coefficients is realized for scales between 1 and 10. Here the scale parameter is proportional with the reciprocal of the frequency. Therefore, each scale can be interpreted as the frequency value, so the lowest scales are related to the high frequencies while the largest ones are due to the low frequencies. As a result, the scale 10 is proportional with the half of the sampling frequency, namely 100 Hz. However this three dimensional figure can be reduced to two dimensional plane and then, it can be represented as time-scale plane (Fig. 5).

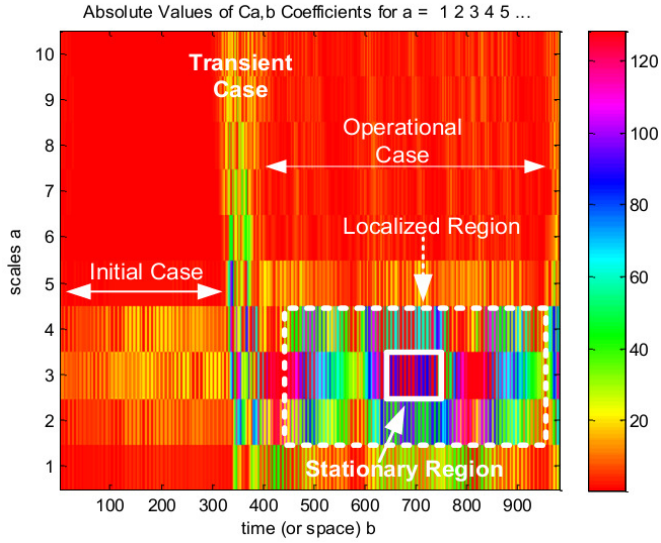

Fig. 5. Time-scale representation of the CWT (time = b × 0.005 s)

Fig. 5 indicates similar properties, which are observed in Fig. 4. However, the time and scale properties are clearer than the previous one. In this manner, huge amplitudes are localized between the scales 1 and 5 in time interval defined between 1.8 and 5 seconds (for b = 360 and 1000 in Figure 5). This region covers the operation region of the current signal as indicated in Fig. 1. However, this region still reflects the non-stationary signal characteristics. In order to extract the stationary region of the signal, if more localized region defined at around scale 3 and between 3.2 and 3.7 seconds (for b = 640 and 740 in Fig. 5) is considered, this time-scale part can be represented as a stationary signal as shown in Fig. 6(a) as well as its PSD given in Fig. 6(b).

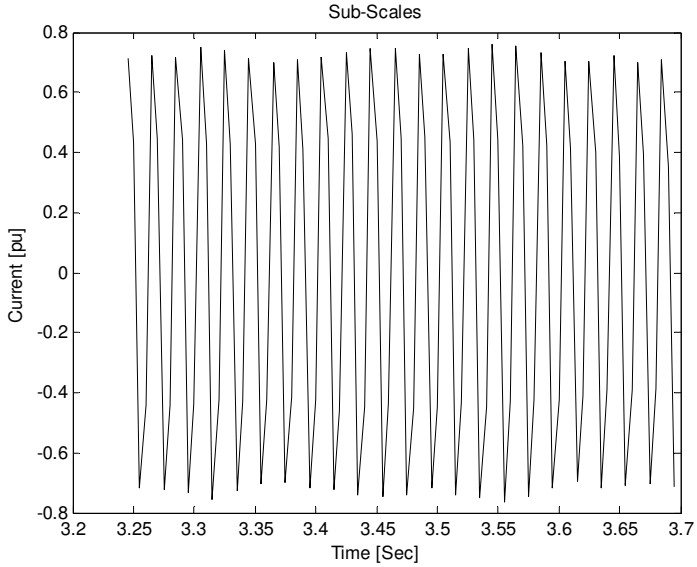

(a)

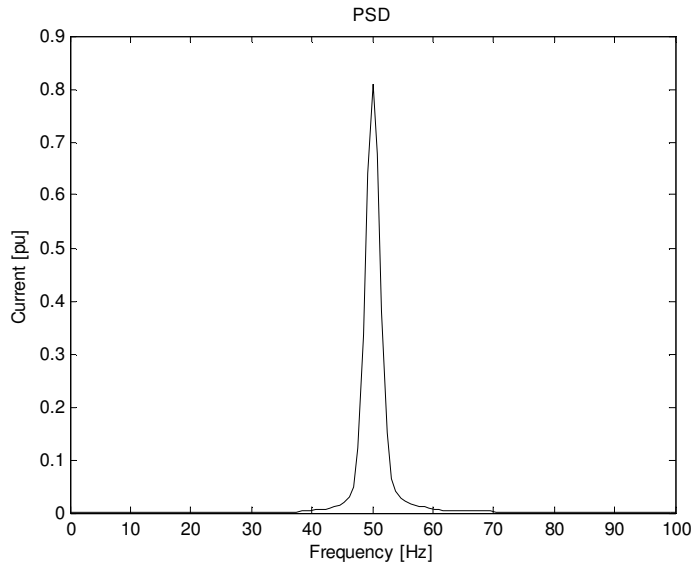

(b)

Fig. 6. Sinusoidal waveform as a feature extracted from the welter current:
a) Stationary signal in time domain, b) PSD of the stationary signal

Hence, the extracted feature from the non-stationary current signal of the welding machine is defined as a sinusoidal waveform of 50 Hz. Here duration of this feature can be interpreted as welding period.

5. Concluding remarks

In this study, current signals of an electrical welding machine are taken through the measurement system based on Hall effect sensor. Here, the sampling frequency is 200 Hz (sampling time is 0.005 s). In terms of the mathematical methods, Continuous Wavelet Transform (CWT) and Power Spectral Density (PSD) approaches are applied. Results of the analysis may be summarized as follows:

- A sinusoidal waveform at fundamental frequency of 50 Hz is strongly localized between 3.2 (b = 640) and 3.7 (b = 740) seconds.
- The side bands of the fundamental frequency can be shown by the scale 2 and 4 appearing at around scale 3 and they appear along the overall time.
- Transient case contains all frequency band between the 0-100 Hz after the 1.6 sec. (b = 320 in Fig. 5).

Consequently, the sinusoidal component of the welding current is localized at 50 Hz within very short time (0.5 second) can be interpreted as stationary signal characteristic of the welding current signal and hence it denotes the welding period with perfect contact between the welding electrode and material surface. In this sense, this research is an original study in terms of the application area of the welding, considering the wavelet transform technique, the Hall sensor-based data acquisition system and the extraction of the stationary signal characteristics.

Acknowledgement

Author presents his special thanks to Dr. Gokhan Gokmen and all people in the Welding Laboratory of Technology Faculty at Marmara University for their valuable contributions in providing of the data used in this research.

References

[1] www.millerwelds.com/interests/instructors/pdf/Electrical_Fundamentals.pdf, (Feb. 2010).
[2] **John E. H.** Measurement of electrical parameter of AC arcs. IEEE Transactions on Industry and General Applications, September/October 1969, Vol. IGA-5, No. 5.
[3] **Hao X., Song G.** Spectral analysis of the plasma in low-power laser/arc hybrid welding of magnesium alloy. IEEE Transactions on Plasma Science, 2008.
[4] **Karen R.** Welding Basics: An Introduction to Practical & Ornamental Welding. Creative Publishing International Inc., Minnesota, ISBN 1-58923-139-2, 2004.
[5] **Lancaster J. F.** The Physics of Welding. Pergamon Press, 1984.
[6] http://www.ehow.com/about_4661176_electric-welding-machines.html, (Feb. 2010).
[7] **Akinci T. Ç., Nogay H. S., Gokmen G.** Determination of optimum operation cases in electric arc welding machine using neural network. Springer Journal of Mechanical Science and Technology, Vol. 25, No. 4, 2011, p. 1003-1010.
[8] **Akinci T. Ç.** Time - frequency analysis of the current measurement by Hall effect sensors for electric arc welding machine. Mechanika, No. 5, Vol. 85, 2010, p. 66-71.
[9] **Palanco S., Klassen M., Skupin J.** Spectroscopic diagnostics on CW - laser welding plasmas of aluminum alloys. Spectrochim. Acta B, At. Spectrosc., Vol. 56, No. 6, June 2001, p. 651-659.
[10] **Mirapeix J., Cobo A., Conde O. M., Jauregui C., Lopez-Higuera J. M.** Real-time arc welding defect detection technique by means of plasma spectrum optical analysis. NDT&E Int., Vol. 39, No. 5, July 2006, p. 356-360.
[11] **Hao X., Song S.** Spectral analysis of the plasma in low-power laser/arc hybrid welding of magnesium alloy. IEEE Transactions on Plasma Science, 2008.

[12] **Luo H., Zeng H., Hu L., Hu X., Zhou Z.** Application of artificial neural network in laser welding defect diagnosis. Elsevier Journal of Materials Processing Technology, Vol. 170, 2005, p. 403-411.

[13] **Groslier D., Pellerin S., Valensi F., Richard F., Briand F.** Explorative approach of the spectral analysis tools to the detection of welding defects in lap welding. Taylor & Francis, Nondestructive Testing and Evaluation, 2010, p. 1-21.

[14] **Slania J.** Use of Fourier transforms in analysis of pulsed MAG welding. Welding International, Vol. 11, No. 10, 1997, p. 761-764.

[15] **Thamodharan M., Beck H. P., Wolf A.** Steady and pulsed direct current welding with a single converter. Welding Research, 1999, p. 45-79.

[16] **Sorensen C. D., Eagar T. W.** Measurement of oscillations in partially penetrated weld pools through spectral analysis. Journal of Dynamic Systems, Measurement and Control - Transactions of the ASME, Vol. 112, September 1990, p. 463-468.

[17] **Wang J. F., Chen B., Chen H. B., Chen S. B.** Analysis of arc sound characteristics for gas tungsten argon welding. Sensor Review, Emerald Group Publishing Ltd., Vol. 29, No. 3, 2009, p. 240-249.

[18] **Vaseghi S. V.** Advanced Signal Processing and Digital Noise Reduction. John Wiley & Sons Inc., 1996.

[19] **Seker S.** Determination of air-gap eccentricity in electric motors using coherence analysis. IEEE Power Engineering Review, Vol. 20, No. 7, 2000, p. 48-50.

[20] **Taskin S., Seker S., Karahan M., Akinci T. Ç.** Spectral analysis for current and temperature measurements in power cables. Electric Power Components and Systems, Vol. 37, Issue 7, 2009, p. 415-426.

[21] **Azzoni D., Rüdiger B., Michael F., Harmut G., Hans-Dieter H., Jürgen K., Andreas N., Alfred V.** Isolated current and voltage transduser characteristic – applications - calculations, September 20-22, LEM Coporate Communications, Genova, 1999.

[22] **Gilbert J., Dewey R.** Application Information. Application Note 27702A, Allegro Microsystem Inc., p. 1-12.

[23] Amploc current sensors. Engineering Reference Book, 2002, p. 1-8.

[24] Allegro Microsystem Inc. Data Sheet 27501.10B. 3515 and 3516 Ratiometric Linear Hall-Effect Sensors, 2001, p. 1-10.

[25] Magnetics Division of Spang & Company. Magnetics Cores for Hall Effect Sensors, Technical Bulletin Hed-01, 2001, p. 2-6.

[26] Magnetics Division of Spang & Company. Design Application Notes, Power Design Section 4, p. 12-13.

[27] **G. Gökmen** Design and Calibration of Electronic Current Transformer, Ph. D. Thesis of Applied Science in Electrical Education, Institute of Pure and Applied Sciences, Marmara University, May 2006.